Two variants of the major serine protease inhibitor from the sea anemone *Stichodactyla helianthus*, expressed in *Pichia pastoris*

Rossana García-Fernández [a, *], Patrick Ziegelmüller [b], Lidice González [a], Manuel Mansur [c], Yoan Machado [d, 1], Lars Redecke [e], Ulrich Hahn [b], Christian Betzel [b], María de los Ángeles Chávez [a, **]

[a] *Centro de Estudio de Proteínas, Facultad de Biología, Universidad de la Habana, Cuba*
[b] *Institute of Biochemistry and Molecular Biology, Department of Chemistry, Faculty for Mathematics Informatics and Natural Sciences, University of Hamburg, Germany*
[c] *Elanco Animal Health, Greenfield, IN, USA*
[d] *Centro de Inmunología Molecular, La Habana, Cuba*
[e] *Institute of Biochemistry, Center for Structural and Cell Biology in Medicine, University of Lübeck, Germany*

ARTICLE INFO

ABSTRACT

The major protease inhibitor from the sea anemone *Stichodactyla helianthus* (ShPI-1) is a non-specific inhibitor that binds trypsin and other trypsin-like enzymes, as well as chymotrypsin, and human neutrophil elastase. We performed site-directed mutagenesis of ShPI-1 to produce two variants (*r*ShPI-1/K13L and *r*ShPI/Y15S) that were expressed in *Pichia pastoris*, purified, and characterized. After a single purification step, 65 mg and 15 mg of protein per liter of culture supernatant were obtained for *r*ShPI-1/K13L and *r*ShPI/Y15S, respectively. Functional studies demonstrated a 100-fold decreased trypsin inhibitory activity as result of the K13L substitution at the reactive (P1) site. This protein variant has a novel tight-binding inhibitor activity of pancreatic elastase and increased activity toward neutrophil elastase in comparison to *r*ShPI-1A. In contrast, the substitution Y15S at P2′ site did not affect the K_i value against trypsin, but did reduce activity 10-fold against chymotrypsin and neutrophil elastase. Our results provide two new ShPI-1 variants with modified inhibitory activities, one of them with increased biomedical potential. This study also offers new insight into the functional impact of the P1 and P2′ sites on ShPI-1 specificity.

© 2016 Elsevier Inc. All rights reserved.

1. Introduction

Kunitz-type protease inhibitors belonging to the Bovine Pancreatic Trypsin Inhibitor (BPTI) family (PFAM: PF00014) are among the most extensively studied protein-protein binding systems. Site-directed mutagenesis studies of this family have mainly focused on mammalian proteins, such as BPTI [1—4]. Furthermore, most studies have focused on the reactive residue, the P1 site according to the Schechter and Berger notation, which is the main contributor to the binding association energy and specificity [5,6]. Typical trypsin inhibitors have Arg/Lys at this P1 site whereas chymotrypsin inhibitors have aromatic residues, Leu or Met, and elastase inhibitors usually contain aliphatic reactive residues at this position [1,7]. The functional impact of other positions has been also studied through site-directed mutagenesis but mainly on the Pn side (P5—-P1 sites) of the binding loop [8].

We have previously reported the purification, characterization and recombinant expression of a BPTI-Kunitz type inhibitor, isolated from the sea anemone *Stichodactyla helianthus* (ShPI-1, UNI-PROT ID: P31713) [9]. Wild-type ShPI-1 bears a basic residue at the P1 site, which explains its activity mainly toward trypsin-like enzymes, such as trypsin, kallikrein and plasmin. Like the Lys (P1)-containing inhibitor BPTI, ShPI-1 is able to bind chymotrypsin and human neutrophil elastase (HNE) [10,11]. The presence of Tyr15 at P2′ position of ShPI-1 is suggested to support these activities [9], taking into account the hydrophobic nature of their S2′ pockets. Nevertheless, the impact of this hydrophobic residue on the activity of ShPI-1 has been not tested by site-directed mutagenesis. Other remarkable activities of ShPI-1 include its unusual ability to interact with cysteine and aspartic proteases and the strong inhibition of other serine proteases, such as kallikrein, plasmin and HNE [9]. Together with its novel functional features, ShPI-1 has potential applications in biotechnology [12,13] and in biomedicine, the latter as a result of its antiparasitic effect against trypanosomatids [14,15]. These facts emphasize the importance of understanding the functional determinants of ShPI-1 and of characterizing new variants with different specificities or higher selectivity toward enzymes of biomedical interest.

Here we report the site-directed mutagenesis of ShPI-1 at the P1 and P2′ sites resulting in two variants named *r*ShPI-1/K13L and *r*ShPI-1/Y15S. Both recombinant proteins were expressed in *Pichia pastoris* and purified. Kinetic studies demonstrated their modified specificity and inhibitory strength, in comparison with the pseudo wild-type inhibitor *r*ShPI-1A that is produced in the same host [12]. This is the first report describing mutagenesis at different positions of ShPI-1 and its functional effect on the activity against nine serine proteases. Modification at the P1 site reduced binding to trypsin-like enzymes and significantly increased the inhibitor selectivity toward elastases. The functional effect of mutation at P2′ site, initially designed to decrease inhibition of chymotrypsin, was lower than expected. Thus, the hydrophobic residue Tyr15 may not has a great influence into chymotrypsin binding, which suggests that other positions should be studied.

2. Materials and methods

2.1. Strains and molecular biology reagents

Escherichia coli TOP10 and *Pichia pastoris* KM71H strains, both from Invitrogen (USA), were used as cloning and expression hosts systems, respectively. Restriction enzymes, DNA ligase, *Taq* (*Thermus aquaticus*) and *Phusion*™ (*Pyrococcus* sp.) polymerases and their buffers, were obtained from Fermentas (Germany) or NEB (USA).

2.2. Cloning and site-directed mutagenesis

The gene of wild-type ShPI-1 was amplified by PCR using as a template the plasmid pBM301 that contains the gene of the pseudo wild-type inhibitor ShPI-1A [12]. A first PCR was performed with site specific primers to eliminate the additional residues on the *r*ShPI-1A gene [12]. The sense primer (5′-TCTCTCGAGAAAA-GA**TCCATCTGCAGCGAACCG**-3′) included the 5′ end of the ShPI-1 gene that encodes for amino acids 1 to 6 (bold letters), an *Xho*I restriction site, and the recognition site of the Kex2 enzyme. The antisense primer (5′-TGTTCTAGATTACTA**CGCGCGGCAGATAGC**-3′) hybridized at the 3′ end of the ShPI-1 gene that encodes amino acids 51–55 (bold letters) and additionally includes two stop codons and an *Xba*I restriction site. The PCR mixture (50 μL) contained 100 μM dNTPs, 0.5 μM each primer, 40 ng of template and 0.5 U of *Taq* DNA polymerase. The program [$1 \times$ (2 min, 95 °C); $20 \times$ (30 s,

95 °C; 45 s, 72 °C); $1 \times$ (5 min, 72 °C); 1×20 °C] was performed in a *Mastercycler*® (Eppendorf, Germany). The purified product was cloned into the *Xho*I/*Xba*I-digested pPICZαA vector (Invitrogen, USA). The resultant vector (pPICSh) was used as template for the site-directed mutagenesis following the standard Quick Change method (Stratagene, USA) using the primers shown in Table 1. Mutagenesis was performed in 50 μl of the supplied GC buffer, 5–10 ng template, 0.2 μM each primer, 200 μM dNTPs and 1U of Phusion DNA polymerase. After the initial denaturation step at 98 °C for 30 s, the mutagenesis reaction was conducted for 30 cycles with denaturation at 98 °C for 10 s, primer annealing at Tm+3 °C for 30 s and DNA synthesis at 72 °C for 2 min, with a final extension at 72 °C during 5 min. The final product was digested with 10U of *Dpn*I for 90 min at 37 °C before transformation of *E. coli* TOP10 cells by plasmid electroporation. Resulting vectors were sequenced at the University Medical Center Hamburg (Germany).

2.3. Production of rShPI-1/K13L and rShPI-1/Y15S

Transformation of *Pichia pastoris* and further analysis were performed according to the Easy Select *Pichia* Expression Kit (Invitrogen, USA). *P. pastoris* strains for production of *r*ShPI-1/K13L and *r*ShPI-1/Y15S were isolated by increasing concentrations of zeocine in the culture media up to 100 μg/mL. The pseudo wild-type inhibitor *r*ShPI-1A and the *r*ShPI-1/K13L variant were produced in a 1.5 L fermenter as previously reported [12]. The variant *r*ShPI-1/Y15S was produced using a similar protocol and after 48 h of culture at 28 °C and 200 rpm, the cells were harvested by centrifugation, inoculated in 150 mL minimal medium [9] and further incubated for 72 h at 28 °C with the addition of 1% (v/v) methanol every 24 h. Protein secretion to the medium was evaluated by SDS-PAGE [14] and Western-blotting. The inhibitory activities against pancreatic trypsin (EC 3.4.21.4) and chymotrypsin (EC 3.4.21.1) were tested using the substrates Bz-Arg-pNA [15] or Suc-Ala-Ala-Pro-Phe-pNA [16], respectively (Table 2).

Protein purification from culture supernatants was performed in a Streamline Direct HST-1 multi-modal resin, as previously reported [12]. Protein concentrations were estimated by measuring the absorbance at 280 nm, using the specific extinction coefficient of ShPI-1 (E_{280} 1% = 5.2) [9]. The integrity and identity of the proteins was verified by molecular mass determination and peptide mapping, as further described.

2.4. Immunodetection of the recombinant proteins

Immunodetection was performed using a polyclonal antibody against the pseudo wild-type inhibitor *r*ShPI-1A generated in a BalB/C mouse (unpublished). The serum was diluted 1:5000 in 0.1% (m/v) bovine serum albumin and dissolved in Tris-buffered saline (TBS). An alkaline phosphatase conjugated anti-mouse IgG was used as secondary antibody and the reaction was visualized using Nitro Blue Tetrazolium (0.1%) and 5-bromo-4-chloro-3-indolyl phosphate (0.5%) in Tris-HCl, pH 9.5.

2.5. Peptide mapping and molecular mass determination

Proteins were treated with 40 mM dithiothreitol (DTT) for 1 h at 37 °C and the reduced Cys residues were modified with iodoacetamide or acrylamide (100 mM) by incubation in the dark for 30 min at 37 °C. Subsequently, the variant *r*ShPI-1/K13L was digested with trypsin and *r*ShPI-1/Y15S with endoproteinase Glu-C (*Staphylococcus. aureus* V8) or a Glu-C/lysil endopeptidase (LEP) mixture (1:1), for 2 h at 37 °C. Mass spectroscopy was done on a MALDI-TOF-TOF Axima Performance mass spectrometer (Shimadzu, Japan), equipped with a 337 nm pulsed nitrogen laser.

Table 1
Oligonucleotides used for site-directed mutagenesis of ShPI-1.

```
 1  2  3  4  5  6  7  8  9 10 11 12 13 14 15 16 17 18

SerIleCysSerGluProLysLysValGlyArgCysLysGlyTyrPheProArg

tccatctgcagcgaaccgaaaaaagtcggccgttgcaaaggttacttcccgcggtt
```

Primer	Sequence	Lenght (nt)	Tm (°C)
K13L_fw	gtcggccgttgcCTaggttacttcccg	28	75.4
K13L_rv	cgggaagtaacctAGgcaacggccgac	28	75.4
Y15S_fw	cgttgcaaaggAaGCttcccgcggttc	27	69.7
Y15S_rv	gaaccgcgggaaGCtTcctttgcaacg	27	69.7

Table 2
Conditions used for enzyme kinetic assays.

Enzyme	[E₀] (M or U)[a,b]	Substrate [Reference]	[S₀] (mM)[a]	Buffer
Porcine pancreatic trypsin	$2.2 \cdot 10^{-7}$	Bz-Arg-pNa [15]	1.0 ($1 K_M$)	20 mM Tris-HCl; 150 mM NaCl; 20 mM CaCl₂; pH 8.0
Porcine pancreatic kallikrein	$5.4 \cdot 10^{-7}$	HD-Val-Leu-Arg-pNA [58]	0.5 ($1 K_M$)	50 mM Tris-HCl; 16 mM NaCl; pH 7.8
Human plasmin	$2.4 \cdot 10^{-8}$	HD-Val-Leu-Lys-pNA [59]	0.4 ($1 K_M$)	50 mM Tris-HCl; 110 mM NaCl; pH 7.4
Human factor Xa	0.1 U	Bz-Ile-Glu-Gly-Arg-pNA [60]		50 mM Tris-HCl; 13 mM NaCl; 20 mM CaCl₂; pH 8.3
Human thrombin	1 U	HD-Phe-Pip-Arg-pNA [19]	0.4 ($1 K_M$)	50 mM Tris-HCl; 130 mM NaCl; 20 mM CaCl₂; pH 8.3
Bovine pancreatic chymotrypsin	$2.8 \cdot 10^{-8}$	Suc-Ala-Ala-Pro-Phe-pNA [16]	1.0 ($1 K_M$)	50 mM Tris-HCl; pH 8.0
Human neutrophil elastase (HNE)[2]	$1.0 \cdot 10^{-7}$	MeOSuc-Ala-Ala-Pro-Val-pNA [20]	0.14 ($1 K_M$)	20 mM Tris-HCl; 500 mM NaCl; pH 8
Porcine pancreatic elastase (PPE)	$3.3 \cdot 10^{-8}$	Suc-Ala-Ala-Ala-pNA [20]	0.7 ($0.7 K_M$)	30 mM Sodium Phosphate; 50 mM NaCl; pH 7.0
B. licheniformis subtilisin	$2.3 \cdot 10^{-9}$	Suc-Ala-Ala-Pro-Phe-pNA [21]	0.12 ($1 K_M$)	100 mM Tris-HCl; 0.1% Triton X-100; pH 8.6

[a] Concentrations in the assays (M: mol/L).
[b] Abbreviations: [Eo]: enzyme concentration, [So]: substrate concentration, K_M: Michaelis constant, U: activity units. One unit of enzymatic activity was defined as the amount of enzyme able to hydrolyze 1 μmol of substrate per min under the specified conditions.

Samples were desalted in ZipTipC18 reverse-phase microcolumns and mixed with equal volumes of α-cyano-4-hydroxycinnamic acid matrix solution (10 mg/mL in 60% (v/v) acetonitrile and 0.1% (v/v) trifluoracetic acid.) Spectra were acquired in the linear positive ion mode, using 19 kV acceleration voltage. Molecular masses of intact proteins were compared with the theoretical values calculated with the ProtParam analysis tool of the ExPASy server [17], whereas the program MassLynx (Micromass, UK) was used to predict the molecular masses of the expected peptides considering the specificity of the proteolytic enzymes used.

2.6. Circular dichroism (CD)

Right after purification, all protein preparations were subject to circular dichroism spectroscopy in the far UV region (190—250 nm). CD spectra were recorded at 20 °C using a J-715 spectropolarimeter (Jasco, Germany) equipped with a temperature-regulated sample chamber. Five individual scans were averaged, and the background

spectrum was subtracted. The spectra were acquired with a 20 nm/min scan speed and a step resolution of 0.1 nm.

2.7. Analysis of inhibitors specificity

The specificity of the inhibitors was evaluated against the following serine proteases: trypsin, chymotrypsin, elastase (EC 3.24.21.36) and kallikrein (3.4.21.35) from porcine pancreas, human thrombin (3.4.21.5), coagulation factor Xa (3.4.21.6), plasmin (EC 3.24.21.7), neutrophil elastase (EC 3.4.21.37), and *Bacillus licheniformis* subtilisin A (EC 3.24.21.62). All enzymatic activities (n = 3) were determined under initial velocity conditions as previously described [18—21]. The hydrolysis of the specific substrates (summarized in Table 2) was followed at 25 °C by recording the absorbance at 405 nm every 15 s for 3 min. The inhibitory activities were determined by measuring the residual enzymatic activities after incubating the inhibitors and enzymes for 10—30 min at 25 °C, prior to the addition of the substrates. One unit of inhibitory activity was

defined as the amount of protein needed to inhibit one unit of enzymatic activity, which was defined as the amount of enzyme able to hydrolyze 1 μmol of substrate per min under specified conditions.

2.8. Determination of the inhibition constants (K_i)

The active site concentrations of rShPI-1/Y15S and rShPI-1/K13L were determined using trypsin and chymotrypsin, respectively as titrating enzymes. The former was titrated according to [22]. The active concentration of chymotrypsin was determined using soybean trypsin inhibitor (STI) previously titrated with bovine trypsin. All experiments were performed under conditions of $[E_o]/K_i \geq 100$, and assuming the formation of equimolar enzyme:inhibitor complexes. The active concentration of both protein variants were determined following the procedure described in Ref. [23]. Assay conditions and data about the substrates used are shown in Table 2.

3. Results

3.1. Cloning, production and purification of rShPI-1/K13L and rShPI-1/Y15S

The cloning strategy used a PCR reaction to obtain a gene coding for a protein with an amino acid sequence similar to that of natural ShPI-1 [9] by deleting the additional residues EAEA and LG, previously added at the N- and C-termini of rShPI-1A, respectively [12]. After mutagenesis and transformation into *Pichia pastoris*, the KM71H clones being resistant to the highest concentration of zeocine were isolated for protein production. Following 96 h of cultivation, major protein bands with the expected molecular masses were detected by SDS-PAGE in both culture supernatants (Fig. 1A). Enzyme inhibitory activities characterized by dose-dependent effects were also detected in both culture supernatants (results not shown).

Both inhibitors were purified to homogeneity by a single-step cation-exchange chromatography (Fig. 1B) and the identity of the proteins was confirmed using a polyclonal antibody against rShPI-1A (Fig. 1C). The detection of single peaks in the corresponding

MALDI-TOF MS spectrum (Fig. 2) additionally indicated a high purity grade for the preparations. The molecular mass of 6097.47 Da ($M + H^+$) and 6035.03 Da ($M + H$) were in accordance with the expected values for rShPI-1/K13L (6096.82 Da) and rShPI-1/Y15S (6034.82 Da). These results confirmed the correct processing of the α-factor-ShPI-1 fusion, even in the absence of the motif EAEA, in contrast to previous results with BPTI [24]. According to the mass balance analysis of the purified fractions, we obtained protein yields of 65 mg and 15 mg per litre of yeast culture
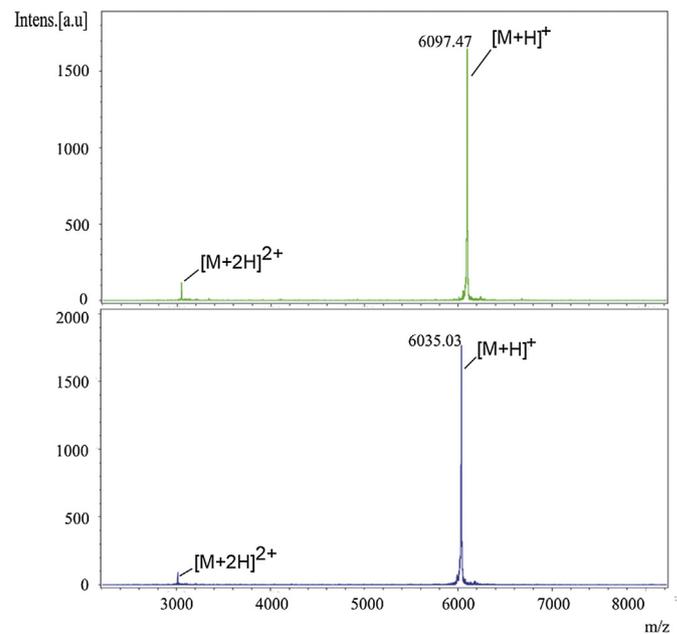

Fig. 2. MALDI-TOF MS spectra of purified rShPI-1/K13L (upper) and rShPI-1/Y15S (bottom). Samples from cation-exchange chromatography were mixed with the matrix solution (α-cyano-4-hydroxycinnamic acid 10 mg/mL in 60% (v/v) acetonitrile and 0.1% (v/v) trifluoroacetic acid) in a 1:10 ratio (v/v) and this mixture (2 μL) was applied on the plate. The species with one $[M+H]^+$ and two $[M+2H]^{+2}$ charges are shown in both spectra.
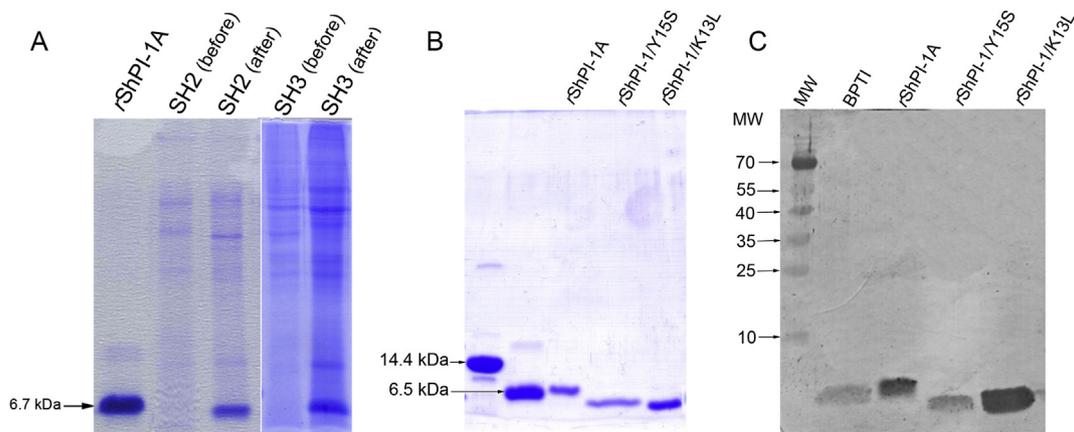

Fig. 1. Production in *P. pastoris* and purification of recombinant ShPI-1 variants. **A)** SDS-PAGE (15%) of culture supernatants of the strains producing the variants rShPI-1/K13L and rShPI-1/Y15S, respectively. Lane 1: the pseudo wild type inhibitor rShPI-1A used as molecular mass marker (6681.6 Da according to [12]); "before", are cultures before induction with methanol and "after" are after 96 h post-induction. **B)** SDS-PAGE (15%) of purified samples. Arrows indicate lysozyme (14.4 kDa) and BPTI (6.5 kDa), used as molecular mass markers. The remaining lanes, from left to right: rShPI-1A and the active fractions from cation-exchange chromatography of rShPI-1/Y15S and rShPI-1/K13L, respectively. Protein bands were visualized by Coomassie Brilliant Blue R-250 staining. **C)** Western-blot of the purified samples using a polyclonal antibody against rShPI-1A. MW: stained molecular mass markers from Fermentas (Germany). BPTI and rShPI-1A were included to indicate the expected positions for the variants rShPI-1/Y15S and rShPI-1/K13L in the purified fractions from cation-exchange chromatography. It should be noted that BPTI was recognized by the antibody, which is probably a consequence of the structural similarities, since these inhibitors share a 33% sequence identity and similar folding [31]. (For interpretation of the references to colour in this figure legend, the reader is referred to the web version of this article.)

supernatant for rShPI-1/K13L and rShPI-1/Y15S, respectively.

3.2. Molecular and conformational characterization of ShPI-1 variants

The amino acid sequences of rShPI-1/K13L and rShPI-1/Y15S were verified by peptide mass mapping using MALDI-TOF MS after specific proteolysis of reduced and cysteine-blocked proteins. This procedure allowed verifying 91% (residues 1–50) of the rShPI-1/K13L amino acid sequence. For rShPI-1/Y15S only 76% of the sequence (residues 14–55) was verified since very short peptides having a similar size range of the matrix signals were obtained from the N-terminal region Ser1-Lys13. For both protein variants, more than one peptide containing the mutated position was detected, thus confirming the amino acids substitutions (Table 3).

As shown in Fig. 3, the circular dichroism spectra of the two proteins variants was similar to that of rShPI-1A. All CD spectra showed the features already reported for this inhibitor and other BPTI-Kunitz type proteins [12,25–29], i.e., a positive band at 190–195 nm, a sharp negative band at 202 nm and a shoulder around 220 nm. This results evidenced that purified preparations of rShPI-1/K13L and rShPI-1/Y15S, contained properly folded Kunitz-type proteins.

3.3. Active site titration of the inhibitors

According to previous studies, ShPI-1 is a tight binding (Ki ≤ 10^{-7} M) protease inhibitor, with the strongest activity towards pancreatic trypsin [9]. Therefore, we used that property to perform titration experiments of the ShPI-1 variants here obtained. As shown in Fig. 4A, the residual trypsin activity decreased linearly when increasing rShPI-1/Y15S concentration, indicating that it tightly binds the enzyme under the experimental conditions used. This result allowed fitting the data of the linear portion of the curve to the best theoretical straight line. Accordance with theory, the x-axis intercept of this linear curve represents the point in which inhibitor and enzyme concentrations are equal ([Et] = [It]), when assuming an equimolar complex [18,30]. This procedure allowed the accurate titration of rShPI-1/Y15S. The retrieved active site concentration (22.4 μM) corresponded to 57% of nominal concentration of the purified molecule.

It was impossible to obtain a similar linear response of the trypsin residual activity when titrating the rShPI-1/K13L variant using the same procedure (results not shown). Such result
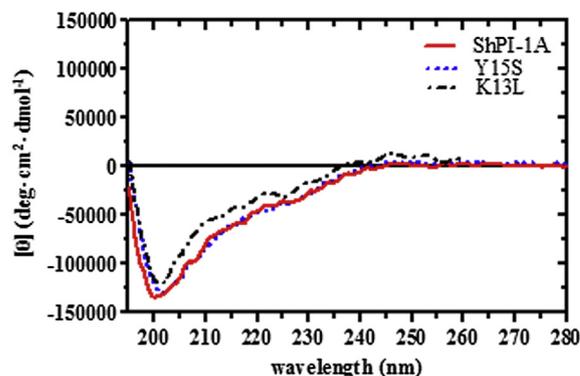

Fig. 3. Far-UV circular dichroism spectra of ShPI-1 variants compared to the pseudo wild-type inhibitor rShPI-1 A. Spectra were recorded just after purification, in 20 mM Tris-HCl, pH 6.5. A scan speed of 50 nm/min and a wavelength step resolution of 0.1 nm were used. Three individual scans were averaged in each experiment, and the background spectra were subtracted.
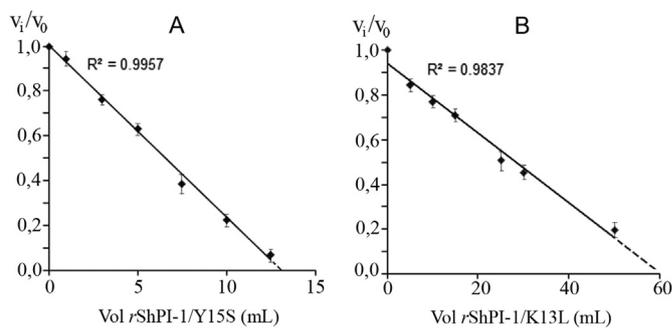

Fig. 4. Determination of the active site concentration of rShPI-1/Y15S (**A**) and rShPI-1/K13L (**B**). v_i/v_0 represents the residual enzymatic activity, in which v_i and v_0 are the activity in presence and in absence of the inhibitor, respectively. Trypsin or chymotrypsin, respectively, were mixed with increasing volumes of the inhibitors and the ratio v_i/v_0 was determined after adding the substrates. The linear portion of each plot of fractional activities versus inhibitor volume was fitted to a line. The active inhibitor concentration was obtained from the intercept with the x axis, which represents the equivalence point where the concentration of inhibitor equals the enzyme. The graphs include the means ± S.D (error bars) of at least three replicates (n = 3) and the R^2 value.

indicated an increment of the Ki value against trypsin for this

Table 3
Results from peptide mass mapping of rShPI-1/K13L and rShPI-1/Y15S variants.

Native ShPI-1
^{1}SICSEPKKVG^{11}RC**KGY**FPRFY^{21}FDSETGKCTP^{31}FIYGGCGGNG^{41}NNFETLHQCR^{51}AICRA

Experimental mass (m + H$^+$)	Theoretical mass (m + H$^+$)	Delta (Da)	Sequence (+modification)
rShPI-1/K13L			
948.473	948.482	0.009	^{1}SICSEPKK^8 + Cam
1260.685	1260.673	0.008	^{1}SICSEPKKVGR^{11} + Cam
1352.747	1352.726	0.021	^{8}KVGRCLGYFPR^{18} + Cam
2242.154	2242.075	0.079	^{9}VGRCLGYFPRFYFDSETGK^{27}
912.454	912.440	0.014	^{12}CLGYFPR^{18} + Cam
2545.39	2545.08	0.31	^{28}CTPFIYGGCGGNGNNFETLHQCR^{50} + Cam
rShPI-1/Y15S			
1637.76	1637.75	0.01	^{14}G**S**FPRFYFDSETGK^{27}
1351.53	1351.59	0.06	^{14}G**S**FPRFYFDSE^{24}
3286.38	3286.47	0.09	^{28}CTPFIYGGCGGNGNNFETLHQCRAICRA^{55} + 4Acm
1891.65	1891.77	0.22	^{28}CTPFIYGGCGGNGNNFE^{44} + 2Acm
1413.66	1413.71	0.05	^{45}TLHQCRAICRA^{55} + 2Acm

Amino acid sequence of native ShPI-1 shown at the upper part and labeled every 10 residues. Replaced residues are shown in bold. The variant rShPI-1/K13L was treated with trypsin and cysteines were carboxymethylated (Cam), whereas rShPI-1/Y15S was digested with LEP and LEP/Glu-C (1:1), cysteines were modified with acrylamide (Acm). Peptides bearing the replacement site are highlighted with a gray background.

protein variant, since the linear behavior is only observed when the K_i value is at least two orders of magnitude lower than the enzyme concentration during the assay [18,30]. We then increased the trypsin concentration to favor the $[E_o]/K_i \geq 100$, but similar results were obtained (results not shown). Therefore, active site titration of *r*ShPI-1/K13L was performed using an alternative strategy that involved the use of chymotrypsin, as described in Materials and Methods. A linear response against this enzyme was obtained (Fig. 4B), suggesting a stronger inhibition capacity compared to that of trypsin. Further determination of the intercept, revealed an active concentration of 54.1 μM, corresponding to 71.6% of purified *r*ShPI-1/K13L.

3.4. Inhibition kinetics of serine proteases by ShPI-1 variants and comparison with rShPI-1A

We have previously characterized the pseudo wild-type inhibitor *r*ShPI-1A in terms of functional specificity [9]. Moreover, its K_i value against trypsin was determined by mimicking the experimental conditions used for natural ShPI-1, which involved using the linear Henderson plot [9,31]. Here, we perform a deeper study of the specificity of *r*ShPI-1A against nine serine proteases. Moreover, we determined all K_i values by using the Morrison equation, which is the currently recommended methodology for direct fitting of the fraction velocity *versus* inhibitor active concentration data [32]. As show in Table 4, the K_i value against trypsin ($2.8 \cdot 10^{-9}$ M) was slightly higher than the one reported using the Henderson plot ($1.9 \cdot 10^{-10}$ M) [12]. These differences do not affect our study that was focused on the comparison of *r*ShPI-1A with two variants *r*ShPI-1/K13L and *r*ShPI-1/Y15S, since the same methodology was applied to determine all K_i values (Table 4).

The replacement of the large basic lysine residue at the P1 site with the smaller hydrophobic leucine residue increased the inhibition potential towards chymotrypsin and elastases (Table 4). Hence, according to K_i values of *r*ShPI-1/K13L, this variant is over 10-fold more potent in the inhibition of HNE then the pseudo wild-type inhibitor *r*ShPI-1A. Given the biomedical importance of HNE, this is a positive result. Moreover, the *r*ShPI-1/K13L variant is a high-affinity PPE inhibitor, as shown by the concave inhibition curve (Fig. 5A) and the K_i value obtained against this enzyme. In contrast, there was no such activity for the pseudo-wild type inhibitor *r*ShPI-1A (Table 4). Inhibition of PPE was stable from the first minute of incubation with *r*ShPI-1/K13L (Fig. 5B), thus indicating that the enzyme, the inhibitor, and the substrate, as well as their complexes, were in equilibrium.

Besides improving the inhibition of elastase like-enzymes, the introduction of a leucine at the P1 site of ShPI-1 impaired the inhibition of trypsin-like enzymes. As shown in Table 4, the trypsin binding affinity of the *r*ShPI-1/K13L variant was significantly decreased (about 100-fold) compared to the wild-type like inhibitor *r*ShPI-1A. In addition, the tight-binding inhibition activity against kallikrein and plasmin observed in *r*ShPI-1A, was not detected for the variant *r*ShPI-1/K13L, despite using high $[I_o]/[E_o]$ molar ratios or increasing the enzyme-inhibitor incubation times (Table 4).

On the other hand, substitution of the hydrophobic tyrosine residue by serine at the P2′ site of ShPI-1 did not cause a substantial change in the specificity of the inhibitor. Hence, the K_i value of the *r*ShPI-1/Y15S variant against trypsin is quite similar to that of the pseudo wild-type molecule *r*ShPI-1A (Table 4). Moreover, the inhibition of HNE was only slightly reduced, as shown by the 10-fold increased real K_i values against this enzyme, compared to *r*ShPI-1A. A similar behavior was observed for the inhibitory activity against chymotrypsin, which was only slightly decreased despite substituting the hydrophobic residue at P2′ site by serine.

4. Discussion

In this work we introduced a leucine at the P1 site of the *Stichodactyla helianthus* protease inhibitor ShPI-1, to favor the inhibition of elastases-like enzymes. We also evaluated the effect of a serine at the P2′ site, to evaluate its effect on the chymotrypsin inhibition. Two *P. pastoris* strains expressing high amounts of *r*ShPI-1/K13L and *r*ShPI-1/Y15S were produced, and we demonstrated the functional effect of these substitutions on the inhibitory activity against nine serine proteases.

4.1. Correct processing and high production levels of two ShPI-1 variants in Pichia pastoris

According to mass spectra and peptide mass mapping, the secreted proteins *r*ShPI-1/Y15S and *r*ShI-1/K13L were homogeneous at their N-terminal region. This result demonstrated the correct processing of the α-factor-*r*ShPI-1 fusion, despite eliminating the N-terminal Glu-Ala-Glu-Ala tag previously added during expression of the pseudo wild-type inhibitor *r*ShPI-1A. Since this tag mimics the Pn′ sites of the Golgi Kex2p subtilase target region, it is usually included to favor correct processing of recombinant proteins produced in yeast by using the prepro leader peptide of alpha mating factor (AMF) [24,33—35]. When absent, for example, during production of *r*BPTI with the natural Arg-Pro-Asp N-terminal, several "isoforms" with a variability of 4—11 amino acids at the extension site are produced. In contrast, inclusion of the spacer DNA encoding Glu-Ala before the N-terminus leads to the secretion

Table 4
Specificity and K_i values of ShPI-1 variants against serine proteases.

Enzyme	Natural ShPI-1 [10]	*r*ShPI-1A	*r*ShPI-1/K13L	*r*ShPI-1/Y15S
Pancreatic trypsin	*1.3·10⁻¹⁰*	*[12] 5.6·10⁻¹⁰* 2.75·10⁻⁹	3.2·10⁻⁷ ↓	5.0·10⁻⁹
Pancreatic kallikrein	*8.5·10⁻⁸*	1.46·10⁻⁸	N.i	+
Human plasmin	*2.7·10⁻⁹*	4.42·10⁻⁹	N.i	+
Human factor Xa		N.i.		
Human α-thrombin		N.i.		
Pancreatic chymotrypsin	*2.3·10⁻⁹*	1.48·10⁻⁸	4.5·10⁻⁹ ↑	1.35·10⁻⁷ ↓
Neuthrophil elastase	+	2.35·10⁻⁸	1.3·10⁻⁹ ↑	1·10⁻⁷
Pancreatic elastase	N.i.	N.i.	1.2·10⁻⁸	N.i
Subtilisin	N.i.	N.i.	N.i.	N.i

All values are expressed in mol/L. The K_i values shown in italics were previously determined using the Henderson Plot, whereas remaining values were determined in the current work using the Morrison equation, which is currently the recommended method; + indicates a positive inhibition effect for which K_i values were not determined. Arrows are used to show if the inhibition strength were increased (↑) or reduced (↓), compared to those of *r*ShPI-1A (lower K_i values indicate higher inhibition strengths). N.i. means that not inhibition was detected, even applying high I_o/E_o molar ratios and incubation times up to 30 min. Empty spaces indicate that the activity has not been tested.
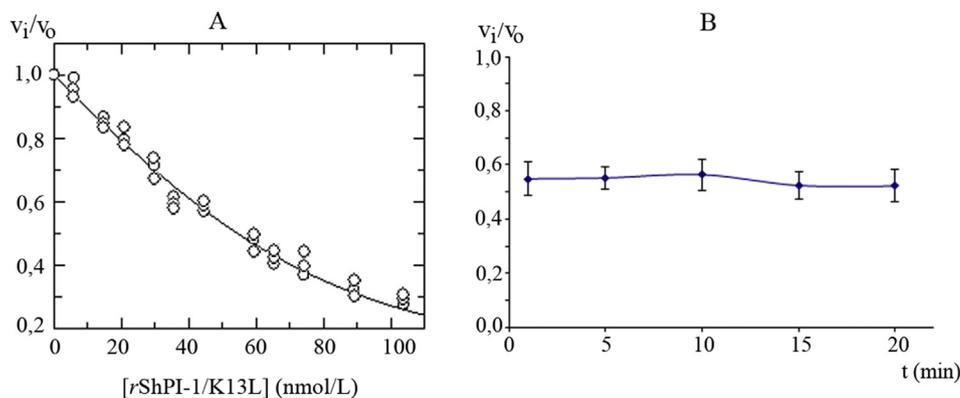
Fig. 5. Kinetic characterization of the interaction between rShPI-1/K13L and pancreatic elastase. **A**) Determination of the dissociation constant (K_i). A constant concentration of PPE (35 nM) was mixed with increasing amounts of the inhibitor (6–104 nM), and the residual enzyme activity was determined. v_i/v_o represents the fractional activity in presence (v_i) and in absence of inhibitor (v_o). The connecting line represents the best fit to the quadratic Morrison's equation for tight binding inhibitors. **B**) Time dependence of the interaction between PPE and rShPI-1/K13L. The enzyme (35 nM) was incubated with 40 nM of the inhibitor during 1, 5, 10, 15 and 20 min at room temperature (30 °C).

of a biologically active BPTI [24]. Nevertheless, as observed here, other BPTI-Kunitz type proteins are obtained with the expected N-terminus even in the absence of this extension [36–38]. It has been shown that variations in Kex2p cleavage efficiency could be different depending on the heterologous protein [39]. Thus, the amino acid at the P1′ position of the Kex2p recognition site—which is the N-terminal residue of the protein if the tag is not included—influences the secretory yield. Hence, the lower production levels of rShPI-1/K13L (65 mg/L) compared to rShPI-1A (1.2 g/L)—although both proteins were produced using similar conditions—could be related to the lack of the Glu-Ala spacer. Differences in the gene copy number, which was here not determined, could also led to differences in the production levels [40–43]. Nevertheless, the yields of rShPI-1/K13L and rShPI-1/Y15S were sufficient to complete the functional characterization.

Purification of the proteins was performed using a cation-exchange chromatography column considering the theoretical isoelectric point of the proteins (8.9 for rShPI-1/Y15S and 8.6 for rShPI-1/K13L). The Streamline Direct HST matrix allowed the efficient capture of the protein despite the high ionic strength of culture supernatants. This approach resulted in pure proteins after a single-step purification as demonstrated by SDS-PAGE and MALDI-TOF MS. The experimental molecular masses obtained for both inhibitor variants and peptide mass mapping confirmed the presence of the single point mutations at the expected positions.

We applied circular dichroism spectroscopy as a sensitive probe of similarity in the overall secondary structure of rShPI-1A and both variants. The minimum seen at 202 nm is unusual for most proteins, but it is a distinctive feature of the BPTI-Kunitz protein family. The shoulder in the CD spectra obtained between 215 and 225 nm is also characteristic for this protein family [25,27]. The negative ellipticity in this region is partly due to the backbone conformations of proline residues at positions 6, 17 and 30 (numbering according natural ShPI-1). These results suggest that the amino acid substitutions didn't affected the overall folding of both proteins variants.

4.2. ShPI-1/K13L and rShPI-1/Y15S: two ShPI-1 variants with modified specificity and inhibitory strength

The pseudo wild-type inhibitor rShPI-1A previously obtained by our group was here submitted to a deeper functional characterization to further demonstrate its similarity with the natural protein. The characterization showed: i) a strong inhibitory capacity towards trypsin and plasmin concurring with the presence of a

basic residue at the P1 site; ii) a relatively lower inhibition activity against kallikrein and no activity toward α-thrombin and factor Xa even using a high [I_o]/[E_o] ratio—this agrees with the strong preference of these enzymes for Arg over Lys at P1 [44–46]; iii) slightly lower binding to HNE and chymotrypsin (K_i 10^{-8} M) compared to binding against trypsin; and, iv) no activity toward PPE. Previous structural studies show that interaction of ShPI-1 with chymotrypsin proceeds through an unusual side chain conformation of the basic P1 site at the entrance of the enzyme S1 pocket (PDB ID: 3OFW, unpublished) also reported for BPTI and APPI [47]. In addition, the hydrophobic residue at the P2′ site of ShPI-1 is suggested to favor inhibition of chymotrypsin, as well as HNE [9]. The structural determinants explaining accommodation of the basic residue in the catalytic pocket of HNE, and not in PPE, are unknown. In this sense, polar desolvation and residue 226 of these enzymes have been suggested to explain such specificity [48].

As expected, the substitution of the basic residue at P1 site of ShPI-1 by leucine affected the activity against trypsin and trypsin-like proteases, i.e., inhibition of kallikrein and plasmin was abolished in the rShPI/1/K13L variant. This inhibitor also showed a reduced activity against pancreatic trypsin, although binding was not abolished. This result was unexpected considering that a similar substitution has a more drastic effect on the activity of BPTI towards trypsin [3]. These differences supported previous suggestions about the contribution of other amino acids, e.g., Arg11 at the P3 site of rShPI-1A, in the stability of its complex with trypsin, [49].

The main effect of the K13L substitution was the generation of inhibitory activity towards PPE, an activity not reported for the natural molecule [9]. This result is consistent with the hydrophobic and shorter size of the S1 pocket in PPE [50]. Moreover, the inhibition capacity of chymotrypsin and HNE was enhanced in the rShPI-1/K13L variant compared to rShPI-1A (Table 4). Elastases catalyze the cleavage of fibrous elastin, which is particularly abundant in the lungs and also present in arteries, skin, and ligaments. Under normal physiological conditions, HNE is tightly controlled by endogenous inhibitors but their affinity is strongly decreased by oxidative stress [51–53]. In this sense, rShPI-1/K13L is an attractive molecule since: i) its serine-protease binding loops do not contain oxidizable residues, and ii) it is a tight-binding inhibitor of elastases and it is more selective than the wild-type molecule. Thus, this protein variant represents a suitable scaffold for further site-directed mutagenesis at positions other than the P1, to improve the inhibitory activity against elastases.

The second variant we obtained, rShPI-1/Y15S, was intended to study the effect of Ser at P2′ site of ShPI-1 and mainly focused on

reducing the inhibition of chymotrypsin. Binding to this enzyme by the wild-type inhibitors BPTI [47] and ShPI-1 (PDB code: 3T62, unpublished) involved an unusual conformation of the basic side chains at their P1 sites. Nevertheless, other BPTI-Kunitz type inhibitors, such as the third domain of SmCI from *Sabellastarte magnifica*, Q8MtR6 from *Haematobia irritans* and CSTI from *Bombyx mori* also contain basic residues at P1 site but not bind chymotrypsin. As a common feature, all these inhibitors contain serine at their P2′ sites [36,54,55]. Likewise, the chymotrypsin inhibition strength of the hepatocyte growth factor activator inhibitor 1B (SPIT-1B or HAI-1B), which contains two BPTI-Kunitz type domains with serine at P2′ sites, is very low (in the mM range) [56]. Hence, we hypothesized that locating Ser at the P2′ site would be deleterious for the inhibition of chymotrypsin, which could be useful to direct the inhibitor selective toward other proteases.

As seen from K_i values of the variant *r*ShPI-1/Y15S, the substitution of a hydrophobic residue at the P2′ site of ShPI-1 decreased the inhibition of chymotrypsin. However, only a 10-fold increase in the K_i value was obtained, thus reducing, but not abolishing, such activity. Similarly to *r*ShPI-1/Y15S, the two BPTI-Kunitz type domains of the hepatocyte growth factor activator inhibitor type 2 (HAI-2, placental bikunin) contain a basic residue (Arg) at the P1 site and Ser at the P2 site; this protein binds chymotrypsin with a K_i value in the nM range [14]. Thus, the assumption of a potential deleterious effect of Ser at the P2′ site on chymotrypsin inhibition may not be the case, or may be influenced by differences in the surrounding residues. Positions at the primary or secondary loops of ShPI-1 and other BPTI-Kunitz type inhibitors could favor or affect the interaction with chymotrypsin. Thus, further site-directed mutagenesis studies are needed to sort this out.

The mutation Y15S variation also reduced binding of HNE, which is consistent with the preference of this enzyme for aromatic residues at P2′ site of substrates/inhibitors [47]. This variant (*r*ShPI-1/Y15S) was active against plasmin and kallikrein, as expected considering the importance of the basic P1 site. Binding to latter might be affected in this protein variant, compared to the wild-type inhibitor, since this enzyme prefers hydrophobic P2′ residues [46]. In contrast, binding to plasmin should not be affected due to its preference at its P2′ sites for Arg, Lys, Ser, or Thr residues [46,57]. These inferences will be tested in future studies.

5. Conclusions

Here we reported the site-directed mutagenesis at P1 and P2′ sites of the protease inhibitor ShPI-1 and the generation of *P. pastoris* strains to produce high levels of two soluble protein variants. Their kinetic characterization, in comparison with *r*ShPI-1A, demonstrated that:

i) the reactive site variant *r*ShPI-1/K13L has a novel inhibition capacity of PPE ($K_i = 1.2 \cdot 10^{-8}$) and slightly enhanced activities against chymotrypsin ($K_i = 4.5 \cdot 10^{-9}$) and HNE ($K_i = 1.3 \cdot 10^{-9}$). Further, binding to trypsin-like proteases was significantly reduced. Thus, the selectivity of ShPI-1 toward elastase-like enzymes was significantly improved, which increases its biomedical potentialities.
ii) the P2′ site variant *r*ShPI-1/Y15S has a 10-fold reduced inhibition activity towards chymotrypsin ($K_i = 1.3 \cdot 10^{-7}$). The presence of a hydrophobic residue at the P2′ site of ShPI-1 is not the main contributor to chymotrypsin binding as previously suggested [9]. Hence, residues at other positions may be contributing to this activity in ShPI-1 and to the lack of activity in similar inhibitors containing serine at this position. This highlights the importance of investigating other positions in order to eliminate chymotrypsin binding, and to improve the selectivity of ShPI-1.

References

[1] D. Krowarsch, M. Zakrzewska, A.O. Smalas, J. Otlewski, Structure-function relationships in serine protease-bovine pancreatic trypsin inhibitor interaction, Protein Peptide Lett. 12 (2005) 403−407.
[2] J.A. Kraunsoe, T.D. Claridge, G. Lowe, Inhibition of human leukocyte and porcine pancreatic elastase by homologues of bovine pancreatic trypsin inhibitor, Biochemistry 35 (1996) 9090−9096.
[3] D. Krowarsch, M. Dadlez, O. Buczek, I. Krokoszynska, A.O. Smalas, J. Otlewski, Interscaffolding additivity: binding of P1 variants of bovine pancreatic trypsin inhibitor to four serine proteases, J. Mol. Biol. 289 (1999) 175−186.
[4] M.A. Salameh, A.S. Soares, A. Hockla, D.C. Radisky, E.S. Radisky, The P(2)′ residue is a key determinant of mesotrypsin specificity: engineering a high-affinity inhibitor with anticancer activity, Biochem. J. 440 (2011) 95−105.
[5] D. Krowarsch, T. Cierpicki, F. Jelen, J. Otlewski, Canonical protein inhibitors of serine proteases, Cell Mol. Life Sci. CMLS 60 (2003) 2427−2444.
[6] I. Schechter, A. Berger, On the size of the active site in proteases. I. Papain. 1967, Biochem. Biophys. Res. Commun. 425 (2012) 497−502.
[7] M. Laskowski Jr., I. Kato, Protein inhibitors of proteinases, Annu. Rev. Biochem. 49 (1980) 593−626.
[8] R. García Fernández, M.L. Reytor, M. Alonso del Rivero, M.A. Chávez, Estudios de relación estructura-función de inhibidores de proteasas tipo BPTI-Kunitz/ Structure-function relationship of BPTI-Kunitz type protease inhibitors, Rev. Cub Cienc. Biol. 4 (2015) 2−19.
[9] J. Delfin, I. Martinez, W. Antuch, V. Morera, Y. Gonzalez, R. Rodriguez, M. Marquez, A. Saroyan, N. Larionova, J. Diaz, G. Padron, M. Chavez, Purification, characterization and immobilization of proteinase inhibitors from Stichodactyla helianthus, Toxicon Off. J. Int. Soc. Toxinol. 34 (1996) 1367−1376.
[10] R. Huber, D. Kukla, A. Ruhlmann, O. Epp, H. Formanek, The basic trypsin inhibitor of bovine pancreas. I. Structure analysis and conformation of the polypeptide chain, Die Naturwiss. 57 (1970) 389−392.
[11] P. Ascenzi, A. Bocedi, M. Bolognesi, A. Spallarossa, M. Coletta, R. De Cristofaro, E. Menegatti, The bovine basic pancreatic trypsin inhibitor (Kunitz inhibitor): a milestone protein, Curr. Protein Pept. Sci. 4 (2003) 231−251.
[12] D.F. Gil, R. Garcia-Fernandez, M. Alonso-del-Rivero, E. Lamazares, M. Perez, L. Varas, J. Diaz, M.A. Chavez, Y. Gonzalez-Gonzalez, M. Mansur, Recombinant expression of ShPI-1A, a non-specific BPTI-Kunitz-type inhibitor, and its protection effect on proteolytic degradation of recombinant human mini-proinsulin expressed in Pichia pastoris, FEMS Yeast Res. 11 (2011) 575−586.
[13] E. Fernandez, J.R. Toledo, M. Mansur, O. Sanchez, D.F. Gil, Y. Gonzalez-Gonzalez, E. Lamazares, Y. Fernandez, F. Parra, O. Farnos, Secretion and assembly of calicivirus-like particles in high-cell-density yeast fermentations: strategies based on a recombinant non-specific BPTI-Kunitz-type protease inhibitor, Appl. Microbiol. Biotechnol. 99 (2015) 3875−3886.
[14] U.K. Laemmli, Cleavage of structural proteins during the assembly of the head of bacteriophage T4, Nature 227 (1970) 680−685.
[15] B.F. Erlanger, N. Kokowsky, W. Cohen, The preparation and properties of two new chromogenic substrates of trypsin, Arch. Biochem. Biophys. 95 (1961) 271−278.
[16] I. Schechter, A. Berger, On the size of the active site in proteases. I. Papain, Biochem. Biophys. Res. Commun. 27 (1967) 157−162.
[17] E. Gasteiger, A. Gattiker, C. Hoogland, I. Ivanyi, R.D. Appel, A. Bairoch, ExPASy: The proteomics server for in-depth protein knowledge and analysis, Nucleic Acids Res. 31 (2003) 3784−3788.
[18] J.G. Bieth, Theoretical and practical aspects of proteinase inhibition kinetics, Methods Enzym. 248 (1995) 59−84.
[19] W. Kisiel, Human plasma protein C: isolation, characterization, and mechanism of activation by alpha-thrombin, J. Clin. Invest. 64 (1979) 761−769.
[20] K. Nakajima, J.C. Powers, B.M. Ashe, M. Zimmerman, Mapping the extended substrate binding site of cathepsin G and human leukocyte elastase. Studies with peptide substrates related to the alpha 1-protease inhibitor reactive site, J. Biol. Chem. 254 (1979) 4027−4032.
[21] E.G. DelMar, C. Largman, J.W. Brodrick, M.C. Geokas, A sensitive new substrate for chymotrypsin, Anal. Biochem. 99 (1979) 316−320.
[22] T. Chase Jr., E. Shaw, p-Nitrophenyl-p′-guanidinobenzoate HCl: a new active site titrant for trypsin, Biochem. Biophys. Res. Commun. 29 (1967) 508−514.
[23] Y. Gonzalez, A.S. Tanaka, I.Y. Hirata, M.A. del Rivero, M.L. Oliva, M.S. Araujo,

M.A. Chavez, Purification and partial characterization of human neutrophil elastase inhibitors from the marine snail Cenchritis muricatus (Mollusca), Comp. Biochem. Physiol. A Mol. Integr. Physiol. 146 (2007) 506–513.

[24] T. Vedvick, R.G. Buckholz, M. Engel, M. Urcan, J. Kinney, S. Provow, R.S. Siegel, G.P. Thill, High-level secretion of biologically active aprotinin from the yeast Pichia pastoris, J. Ind. Microbiol. 7 (1991) 197–201.

[25] P.A. Kosen, T.E. Creighton, E.R. Blout, Circular dichroism spectroscopy of bovine pancreatic trypsin inhibitor and five altered conformational states. Relationship of conformation and the refolding pathway of the trypsin inhibitor, Biochemistry 20 (1981) 5744–5754.

[26] J.A. MacLean 2nd, R.M. Roberts, J.A. Green, Atypical Kunitz-type serine proteinase inhibitors produced by the ruminant placenta, Biol. Reprod. 71 (2004) 455–463.

[27] N. Sreerama, M.C. Manning, M.E. Powers, J.X. Zhang, D.P. Goldenberg, R.W. Woody, Tyrosine, phenylalanine, and disulfide contributions to the circular dichroism of proteins: circular dichroism spectra of wild-type and mutant bovine pancreatic trypsin inhibitor, Biochemistry 38 (1999) 10814–10822.

[28] L. Zhu, J. Wang, J. Mu, H. Wang, C. Zhang, J. Wang, X. Liu, X. Yan, L. Dai, D. Ma, Expression and characterization of Kunitz domain 3 and C-terminal of human tissue factor pathway inhibitor-2, Acta Biochim. Biophys. Sin. (Shanghai) 41 (2009) 948–954.

[29] C. Zhang, D. Kong, X. Liu, X. Yan, L. Dai, D. Ma, Spectroscopic analysis on the effect of temperature on Kunitz domain 1 of human tissue factor pathway inhibitor-2, Acta Biochim. Biophys. Sin. (Shanghai) 39 (2007) 406–412.

[30] C.G. Knight, Active-site titration of peptidases, Methods Enzym. 248 (1995) 85–101.

[31] R. Garcia-Fernandez, T. Pons, A. Meyer, M. Perbandt, Y. Gonzalez-Gonzalez, D. Gil, M. de los Angeles Chavez, C. Betzel, L. Redecke, Structure of the recombinant BPTI/Kunitz-type inhibitor rShPI-1A from the marine invertebrate Stichodactyla helianthus, Acta Crystallogr. Sect. F Struct. Biol. Cryst. Commun. 68 (2012) 1289–1293.

[32] R.A. Copeland, D. Lombardo, J. Giannaras, C.P. Decicco, Estimating KI values for tight binding inhibitors from dose-response plots, Bioorg. Med. Chem. Lett. 5 (1995) 1947–1952.

[33] K.M. Zsebo, H.S. Lu, J.C. Fieschko, L. Goldstein, J. Davis, K. Duker, S.V. Suggs, P.H. Lai, G.A. Bitter, Protein secretion from Saccharomyces cerevisiae directed by the prepro-alpha-factor leader region, J. Biol. Chem. 261 (1986) 5858–5865.

[34] A.S. Xiong, Q.H. Yao, R.H. Peng, P.L. Han, Z.M. Cheng, Y. Li, High level expression of a recombinant acid phytase gene in Pichia pastoris, J. Appl. Microbiol. 98 (2005) 418–428.

[35] T. Kjeldsen, J. Brandt, A.S. Andersen, M. Egel-Mitani, M. Hach, A.F. Pettersson, K. Vad, A removable spacer peptide in an alpha-factor-leader/insulin precursor fusion protein improves processing and concomitant yield of the insulin precursor in Saccharomyces cerevisiae, Gene 170 (1996) 107–112.

[36] M. Alonso-del-Rivero, S.A. Trejo, M.L. Reytor, M. Rodriguez-de-la-Vega, J. Delfin, J. Diaz, Y. Gonzalez-Gonzalez, F. Canals, M.A. Chavez, F.X. Aviles, Tri-domain bifunctional inhibitor of metallocarboxypeptidases A and serine proteases isolated from marine annelid Sabellastarte magnifica, J. Biol. Chem. 287 (2012) 15427–15438.

[37] W.E. Van Nostrand, A.H. Schmaier, R.S. Siegel, S.L. Wagner, W.C. Raschke, Enhanced plasmin inhibition by a reactive center lysine mutant of the Kunitz-type protease inhibitor domain of the amyloid beta-protein precursor, J. Biol. Chem. 270 (1995) 22827–22830.

[38] D. Navaneetham, D. Sinha, P.N. Walsh, Mechanisms and specificity of factor XIa and trypsin inhibition by protease nexin 2 and basic pancreatic trypsin inhibitor, J. Biochem. 148 (2010) 467–479.

[39] S. Yang, Y. Kuang, H. Li, Y. Liu, X. Hui, P. Li, Z. Jiang, Y. Zhou, Y. Wang, A. Xu, S. Li, P. Liu, D. Wu, Enhanced production of recombinant secretory proteins in Pichia pastoris by optimizing Kex2 P1′ site, PLoS One 8 (2013) e75347.

[40] S. Macauley-Patrick, M.L. Fazenda, B. McNeil, L.M. Harvey, Heterologous protein production using the Pichia pastoris expression system, Yeast 22 (2005) 249–270.

[41] M. Mansur, C. Cabello, L. Hernandez, J. Pais, L. Varas, J. Valdes, Y. Terrero, A. Hidalgo, L. Plana, V. Besada, L. Garcia, E. Lamazares, L. Castellanos, E. Martinez, Multiple gene copy number enhances insulin precursor secretion in the yeast Pichia pastoris, Biotechnol. Lett. 27 (2005) 339–345.

[42] Y.Y. Li, K.X. Zhong, A.H. Hu, D.N. Liu, L.Z. Chen, S.D. Xu, High-level expression and characterization of a thermostable xylanase mutant from Trichoderma reesei in Pichia pastoris, Protein Expr. Purif. 108 (2015) 90–96.

[43] H. Yang, C. Zhai, X. Yu, Z. Li, W. Tang, Y. Liu, X. Ma, X. Zhong, G. Li, L. Ma, High-level expression of Proteinase K from Tritirachium album Limber in Pichia pastoris using multi-copy expression strains, Protein Expr. Purif. 122 (2016) 38–44.

[44] H. Czapinska, J. Otlewski, Structural and energetic determinants of the S1-site specificity in serine proteases, Eur. J. Biochem./FEBS 260 (1999) 571–595.

[45] A. Grzesiak, I. Krokoszynska, D. Krowarsch, O. Buczek, M. Dadlez, J. Otlewski, Inhibition of six serine proteinases of the human coagulation system by mutants of bovine pancreatic trypsin inhibitor, J. Biol. Chem. 275 (2000) 33346–33352.

[46] D. Navaneetham, W. Wu, H. Li, D. Sinha, R.F. Tuma, P.N. Walsh, P1 and P2′ site mutations convert protease nexin-2 from a factor XIa inhibitor to a plasmin inhibitor, J. Biochem. 153 (2013) 221–231.

[47] A.J. Scheidig, T.R. Hynes, L.A. Pelletier, J.A. Wells, A.A. Kossiakoff, Crystal structures of bovine chymotrypsin and trypsin complexed to the inhibitor domain of Alzheimer's amyloid beta-protein precursor (APPI) and basic pancreatic trypsin inhibitor (BPTI): engineering of inhibitors with altered specificities, Protein Sci. Publ. Protein Soc. 6 (1997) 1806–1824.

[48] J.E. Hernandez Gonzalez, R. Garcia-Fernandez, P.A. Valiente, Polar desolvation and position 226 of pancreatic and neutrophil elastases are crucial to their affinity for the Kunitz-type inhibitors ShPI-1 and ShPI-1/K13L, PLoS One 10 (2015) e0137787.

[49] R. Garcia-Fernandez, T. Pons, M. Perbandt, P.A. Valiente, A. Talavera, Y. Gonzalez-Gonzalez, D. Rehders, M.A. Chavez, C. Betzel, L. Redecke, Structural insights into serine protease inhibition by a marine invertebrate BPTI Kunitz-type inhibitor, J. Struct. Biol. 180 (2012) 271–279.

[50] W. Bode, E. Meyer Jr., J.C. Powers, Human leukocyte and porcine pancreatic elastase: X-ray crystal structures, mechanism, substrate specificity, and mechanism-based inhibitors, Biochemistry 28 (1989) 1951–1963.

[51] B. Korkmaz, M.S. Horwitz, D.E. Jenne, F. Gauthier, Neutrophil elastase, proteinase 3, and cathepsin G as therapeutic targets in human diseases, Pharmacol. Rev. 62 (2010) 726–759.

[52] S.M. Nobar, M.L. Zani, C. Boudier, T. Moreau, J.G. Bieth, Oxidized elafin and trappin poorly inhibit the elastolytic activity of neutrophil elastase and proteinase 3, FEBS J. 272 (2005) 5883–5893.

[53] H. Carp, A. Janoff, Potential mediator of inflammation. phagocyte-derived oxidants suppress the elastase-inhibitory capacity of alpha 1-proteinase inhibitor in vitro, J. Clin. Invest. 66 (1980) 987–995.

[54] S.S. Azzolini, J.M. Santos, A.F. Souza, R.J. Torquato, I.Y. Hirata, R. Andreotti, A.S. Tanaka, Purification, characterization, and cloning of a serine proteinase inhibitor from the ectoparasite Haematobia irritans irritans (Diptera: Muscidae), Exp. Parasitol. 106 (2004) 103–109.

[55] A. Kurioka, M. Yamazaki, H. Hirano, Primary structure and possible functions of a trypsin inhibitor of Bombyx mori, Eur. J. Biochem./FEBS 259 (1999) 120–126.

[56] D. Kirchhofer, M. Peek, W. Li, J. Stamos, C. Eigenbrot, S. Kadkhodayan, J.M. Elliott, R.T. Corpuz, R.A. Lazarus, P. Moran, Tissue expression, protease specificity, and Kunitz domain functions of hepatocyte growth factor activator inhibitor-1B (HAI-1B), a new splice variant of HAI-1, J. Biol. Chem. 278 (2003) 36341–36349.

[57] M.S. Bajaj, G.I. Ogueli, Y. Kumar, K. Vadivel, G. Lawson, S. Shanker, A.E. Schmidt, S.P. Bajaj, Engineering kunitz domain 1 (KD1) of human tissue factor pathway inhibitor-2 to selectively inhibit fibrinolysis: properties of KD1-L17R variant, J. Biol. Chem. 286 (2011) 4329–4340.

[58] G. Claeson, L. Aurell, P. Friberger, S. Gustavsson, G. Karlsson, Designing of peptide substrates. Different approaches exemplified by new chromogenic substrates for kallikreins and urokinase, Haemostasis 7 (1978) 62–68.

[59] L.E. Mattler, N.U. Bang, Serine protease specificity for peptide chromogenic substrates, Thromb. Haemost. 38 (1977) 776–792.

[60] L. Aurell, R. Simonsson, S. Arielly, G. Karlsson, P. Friberger, G. Claeson, New chromogenic peptide substrates for factor X, Haemostasis 7 (1978) 92–94.